Non-linear wave equations for free surface flow over a bump

Sakaguchi, Shino
Nakayama, Keisuke
Thuy Thi Thu Vu
Komai, Katsuaki
Nielsen, Peter

Non-linear wave equations for free surface flow over a bump

Shino Sakaguchi

Construction Bureau, Kyoto City Hall, Kyoto City, Japan. E-mail: s.vier.no.tn0@gmail.com

Keisuke Nakayama

Department of Civil Engineering, Kobe University, Kobe City, Japan. E-mail: nakayama@phoenix.kobe-u.ac.jp

Thuy Thi Thu Vu

Faculty of Civil Engineering, Thuyloi University, Hanoi, Vietnam. E-mail: thuy.kcct@tlu.edu.vn

Katsuaki Komai

Department of Civil and Environmental Engineering, Kitami Institute of Technology, Kitami City, Japan. E-mail: komai@mail.kitami-it.ac.jp

Peter Nielsen

School of Civil Engineering, University of Queensland, Brisbane, QLD, Australia. E-mail: p.nielsen@uq.edu.au

Abstract

This study aims to develop a new wave equation model by modifying the Fully-nonlinear and strongly-Dispersive Surface wave (FDS) equations. The modification was performed by applying a new expansion in a series of the vertical coordinate, z^{μ}, to the velocity potential while a simple expansion in a series of z was applied to the FDS equations. Verification of the model was conducted by comparing with the theoretical solutions of surface solitary waves. We applied the modified FDS equations to wave fields over a bump under conditions with and without currents, which agreed very well with the time series of wave heights and velocity obtained from laboratory experiments. The dispersion relationship computed using the normalized modified FDS equations also agreed very well with the theoretical solution when we gave the number of expansion terms as 3 with μ=2.5. Additionally, the profile of surface waves computed with the modified FDS equation was shown to have a larger width ridge, a bulbous-type wave, by comparing with a Trochoidal wave under the condition of waves against a current.

Keywords: strongly dispersive, dispersion relationship, bulbous wave, laboratory experiment, variational principle.

1. Introduction

In previous studies, Dean (1965) showed a significant effect of mean currents on the shape of surface waves. Dalrymple (1974) showed the possibility for the existence of a surface wave with a larger width around a ridge under a linear shear condition, which may be a similar condition to a constant current condition. Furthermore, Teles and Peregrine (1988) demonstrated that such a large width ridge wave exists as a "bulbous" wave. The application of a three-dimensional non-hydrostatic model is considered to be one of the solutions to analyze surface waves with current effects playing a significant role in the deformation of surface waves. However, since full three-dimensional non-hydrostatic model costs are very expensive compared to a layer model, it seems necessary to develop a fully-nonlinear layer model that can include current effects but with cheaper runtime.

The system of the Boussinesq-type equations is one of the methods often applied to solve such problems (Mei and Mehaute, 1966; Perigrine, 1967; Madsen and Mei, 1969). An improved Boussinesq-type equation can include a strong dispersive effect with nonlinearity and show high applicability to real scale phenomena (Madsen et al., 1991; Madsen and Sorensen, 1992; Nwogu, 1993; Wei and Kirby, 1995; Wei et al., 1995; Agnon et al., 1999). For example, FUNWAVE is a well-known model which can enable analysis of strong nonlinearity in the near shore region (Wei and Kirby, 1995; Wei et al., 1995). Wei et al. (1999) developed a method for generating waves in the Boussinesq-type equation, such as desired regular and random incident wave with good agreements with laboratory experiments. As a different model application, Zaman et al. (2000) applied the improved Boussinesq equation to analyze surface waves in Nakada Harbor of Okinawa Prefecture, which demonstrated very good agreement with field observations.

However, strong nonlinearity may be important for the analysis of the effects of currents on waves. Nakayama and Kakinuma (2010) developed the Fully-nonlinear and strongly-Dispersive Internal wave (FDI) equation by following Isobe (1995) using the variational principle, which showed that the vertical profile of horizontal velocity under a strong-nonlinear solitary wave can be evaluated accurately. Nakayama and Kakinuma (2010) demonstrated that the FDI equation can reproduce a large amplitude solitary wave with validation using the relationship between wave height and effective wavelength of a solitary wave (Koop and Butler, 1981; Nakayama, 2006). Since the FDI equation was developed under multi-layer conditions (Nakayama and Lamb, 2019), soliton resonance for internal solitary waves (Maxworthy, 1980; Miles, 1997ab;

Tanaka, 1993; Li et al., 2011) and the generation of solitary waves in a tilting tank (Horn et al., 2000; Horn et al., 2001; Horn et al., 2002) can be analyzed successfully (Nakayama et al., 2019a). Furthermore, the solutions obtained using the FDI equation have been applied to give boundary conditions for wave generation, which has been verified from comparisons with the third-order solution of a solitary wave (Nakayama et al., 2012; Nakayama et al., 2019b). Therefore, the Fully-nonlinear and strongly Dispersive Surface wave equations (FDS equation) were developed based on the FDI equation using the characteristic of applicability to a multi-layer system (Nakayama and Kakinuma, 2010; Nakayama et al. (2019a). In the FDI equation, velocity potential is expanded in a series of z, which is used in the FDS equation. To improve the FDS equation, we made an attempt to apply a new expansion in a series of z^{μ}. The improved model is called the modified FDS equation.

Firstly, we applied the modified FDS equation into solitary waves and made comparisons with theoretical solutions by Grimshaw (1971) and Fenton (1972). Secondly, Thuy (2013) carried out laboratory experiments in order to investigate the balance between waves and currents as morphology drivers. We thus applied the modified FDS equation into their laboratory results under wave and wave-current conditions over a bump. Two wave condition cases and one wave-current condition were compared with the modified FDS equation and were verified using a timeseries of surface wave height and a time series of velocity over the bump. The effect of μ was investigated by making comparisons between the FDS equation ($\mu = 1$) and the modified FDS equation ($\mu > 1$) using the normalized modified FDS equation. The effect of an expansion number N on the dispersion relationship was also investigated. Lastly, we investigated the profile of surface waves using Thuy's wave-current laboratory experiments as a fundamental analysis, whether a bulbous wave exists or not under a wave-current condition.

2. Materials and Methods

2.1. *FDS equation*

For the FDS equation (Nakayama et al., 2010; Nakayama et al., 2019a), velocity potential was used to analyze waves using the variational principle of Luke (1967).

$$\boldsymbol{u} = \nabla\phi \text{ and } w = \frac{\partial\phi}{\partial z} \tag{1}$$

where $\boldsymbol{u}$ is the velocity in the horizontal direction, ϕ is the velocity potential, w is the vertical velocity, and ∇ is a partial differential operator in the horizontal plane, i.e., = $(\partial / \partial x, \partial / \partial z)$.

Incompressible fluids are assumed to be stable in still water (Fig. 1). The thickness in still water is denoted by h. The water surface is indicated as η. By following Isobe (1995) based on Luke (1967), the function for the variational problem, F, is determined by

$$F[\phi,\eta] = \int_{t_0}^{t_1} \int \int_A \int_b^\eta \left\{ \frac{\partial \phi}{\partial t} + \frac{1}{2}(\nabla\phi)^2 + \frac{1}{2}\left(\frac{\partial \phi}{\partial z}\right)^2 + gz + \frac{P}{\rho} \right\} \nabla\phi \tag{2}$$

$$P = -\rho g h \tag{3}$$

where g is gravitational acceleration; the plane A, which is the orthogonal projection of the object domain onto the $x - z$ plane is assumed to be independent of time.

In order to derive a set of equations, vertical integration is performed by expanding ϕ into a series in terms of α given a set of vertically distributed functions, Z_α, multiplied by their weightings, f_α.

$$\phi(x,y,t) = \sum_{\alpha=0}^{N-1} Z_\alpha f_\alpha(x,y,t) \tag{4}$$

$$Z_\alpha = z^\alpha \tag{5}$$

where N is the total number of an expanded function.

We substituted Eqs. (4)-(5) into Eq. (2), after the function was integrated vertically. Then the variational principle was applied to obtain the following Euler-Lagrange equations (Eqs. (6) and (7)).

$$Z_\alpha^\eta \frac{\partial \eta}{\partial t} - Z_\alpha^b \frac{\partial b}{\partial t} + \nabla\left(\int_b^\eta Z_\alpha Z_\beta dz \right) \nabla f_\beta - \int_b^\eta \frac{\partial Z_\alpha}{\partial z} \frac{\partial Z_\beta}{\partial z} dz\, f_\beta = 0 \tag{6}$$

$$Z_\beta^\eta \frac{\partial f_\beta}{\partial t} + \frac{1}{2} Z_\beta^\eta Z_\gamma^\eta \nabla f_\beta \nabla f_\gamma + \frac{1}{2} \frac{\partial Z_\beta^\eta}{\partial z} \frac{\partial Z_\gamma^\eta}{\partial z} f_\beta f_\gamma + g\eta + \frac{P}{\rho} = 0 \tag{7}$$

Finally, the FDS equations are

$$\eta^\alpha \frac{\partial \eta}{\partial t} + \frac{1}{\alpha+\beta+1} \nabla\left(\eta^{\alpha+\beta+1} - b^{\alpha+\beta+1}\right) \nabla f_\beta - \frac{\alpha\beta}{\alpha+\beta-1} \nabla\left(\eta^{\alpha+\beta-1} - b^{\alpha+\beta-1}\right) f_\beta = 0 \tag{8}$$

$$\eta^\beta \frac{\partial f_\beta}{\partial t} + \frac{1}{2} \eta^{\beta+\gamma} \nabla f_\beta \nabla f_\gamma + \frac{1}{2} \beta\gamma \eta^{\beta+\gamma-2} f_\beta f_\gamma + g\eta + \frac{P}{\rho} = 0 \tag{9}$$

where α = 0, 1, 2, ..., N-1, β = 0, 1, 2, ..., N-1, and γ = 0, 1, 2, ..., N-1.

104

105 **2.2.** ***Modified FDS equation***

106 In the FDS equation, velocity potential is expanded in a series of z (Eq. (5)), which shows the vertical
107 velocity as Eq. (10). Therefore, the flat bottom boundary condition, $w = 0$ at $z = 0$, cannot be satisfied.

$$w = \frac{\partial \phi}{\partial z} = f_1 + 2f_2 z + 3f_3 z^2 + \cdots + (N-1) f_{N-1} z^{N-2} \tag{10}$$

108 To satisfy the boundary condition automatically, we expanded the velocity potential in a series of z^{μ}.

$$\begin{aligned} \phi(x,y,t) &= \sum_{\alpha=0}^{N-1} z^{\alpha\mu} f_{\alpha}(x,y,t) \\ &= f_0 + z^{\mu} f_1 + z^{2\mu} f_2 + z^{3\mu} f_3 + \cdots + z^{\mu(N-1)} f_{N-1} \end{aligned} \tag{11}$$

109 When $\mu > 1$, the vertical velocity can be given as Eq. (12), which satisfies the flat bottom boundary
110 condition, $w = 0$ at $z = 0$. Also, when we analyze solitary waves, the vertical profile of velocity potential
111 should include a low-order power function of z, such as less than cubic or fourth order. Therefore, it can be
112 suggested that μ should be more than 1 and less than 3 or 4.

$$w = \frac{\partial \phi}{\partial z} = \mu f_1 z^{\mu-1} + 2\mu f_2 z^{2\mu-1} + 3\mu f_3 z^{3\mu-1} + \cdots + \mu(N-1) f_{N-1} z^{\mu(N-1)-1} \tag{12}$$

113 Therefore, the system of new equations, which we call the modified FDS equation, is obtained by
114 substituting Eq. (11) into Eqs. (6) and (7) as follows. It should be noted that the FDS equation can be given
115 when $\mu = 1$.

$$\begin{aligned} &\eta^{\mu\alpha} \frac{\partial \eta}{\partial t} + \frac{1}{\mu(\alpha+\beta)+1} \nabla\left(\eta^{\mu(\alpha+\beta)+1} - b^{\mu(\alpha+\beta)+1}\right) \nabla f_{\beta} \\ &\quad - \frac{\mu^2 \alpha\beta}{\mu(\alpha+\beta)-1} \left(\eta^{\mu(\alpha+\beta)-1} - b^{\mu(\alpha+\beta)-1}\right) f_{\beta} = 0 \end{aligned} \tag{13}$$

$$\eta^{\mu\beta} \frac{\partial f_{\beta}}{\partial t} + \frac{1}{2} \eta^{\mu(\beta+\gamma)} \nabla f_{\beta} \nabla f_{\gamma} + \frac{1}{2} \beta\gamma \eta^{\mu(\beta+\gamma)-2} f_{\beta} f_{\gamma} + g\eta + \frac{P}{\rho} = 0 \tag{14}$$

116 To solve Eqs. (13) and (14), an implicit technique was used in the numerical computational scheme by
117 following Nakayama and Kakinuma (2010).

118

119 **2.3.** ***Validation of modified FDS equation by solitary waves***

120 To verify the application of the modified FDS equation, we applied the model into solitary waves.
121 Grimshaw (1971) and Fenton (1972) developed theoretical solutions, which reproduce surface solitary waves
122 accurately. When a wave height and water depth are given as a_H and h, the wave speed is

$$c_K = \sqrt{gh}\left(1 + \frac{1}{2}\epsilon\right) \tag{15}$$

$$c_F = \sqrt{gh}\left(1 + \epsilon - \frac{1}{20}\epsilon^2 - \frac{3}{70}\epsilon^3\right) \tag{16}$$

$$\epsilon = \frac{a_H}{h} \tag{17}$$

123 where c_K is the wave speed by the KdV theory, and c_F is the wave speed by Fenton (1972).

124 We made comparisons of not only wave speed but also an effective wavelength between the theory and
125 model. The effective wavelength is defined as follows (Koop and Butler, 1981).

$$\frac{\lambda_K}{h} = 2\sqrt{\frac{4h}{3a_H}} \tag{18}$$

$$\lambda_F = \int_{-\infty}^{\infty} \eta_F dx \tag{19}$$

$$\frac{\eta_F}{h} = 1 + \epsilon s^2 - \frac{3}{4}\epsilon^2 s^2\tau^2 + \epsilon^3\left(\frac{5}{8}s^2\tau^2 - \frac{101}{80}s^4\tau^2\right) \tag{20}$$

$$s = \operatorname{sech}\left(\frac{\kappa x}{h}\right) \tag{21}$$

$$\tau = \tanh\left(\frac{\kappa x}{h}\right) \tag{22}$$

$$\kappa = \left(\frac{3}{4}\epsilon\right)^{1/2}\left(1 - \frac{5}{8}\epsilon + \frac{71}{128}\epsilon^2\right) \tag{23}$$

126 where λ_K is the effective wavelength by the KdV theory, λ_F is the effective wavelength by Fenton (1972), and
127 η_F is the surface displacement by Fenton (1972).

128

129 **2.4.** ***Laboratory experiment***

130 The length, width and water depth of an open channel were set to 25.0 m, 1.0 m and 0.5 m, respectively
131 (Fig. 2). A bump with a height of 0.25 m was introduced in the middle of the tank. The length of the bump at
132 the bottom was 3.0 m, and the slope gradient was 1:5 on both sides with a width of 1.0 m. The bump consisted

133 of fine sand with a mean diameter of 0.21 mm. Surface waves were generated using a wave paddle at the left
134 end of Fig. 2, and a wave absorber was located at the right end of Fig. 2. We measured wave height at wave
135 gauge stations using wave gauges, and velocity was measured over a bump (x=8.5 m and z=0.26 m) using an
136 Acoustic Doppler Velocimeter (ADV). Wave height was measured at wg1 (x=0 m), wg2 (x=0.55 m), wg3
137 (x=8.5 m), wg4 (x=7.0 m), and wg5 (x=9.0 m), in which the wave height at wg1 was used as a boundary
138 condition for wave generation.

139 We carried out three laboratory experiments: Case 1 and Case 2 for waves without current, and Case 3 for
140 waves with current. It should be noted that each case has different measurements of wave height and velocities
141 (Table I). Wave height and wave period conditions were 0.10 m and 1.0 s (Case 1) and 0.14 m and 1.5 s (Case
142 2) for surface wave case without current. In Case 1, wave height was measured at wg2 and wg3, and horizontal
143 and vertical velocities were measured at wg3. In Case 2, wave height was measured at wg3 and wg4, and
144 horizontal velocity was measured at wg3. In addition to the above mentioned two cases, we carried out
145 laboratory experiments under the condition of 0.10 m and 1.0 s by giving a 0.02 m/s opposing current, which
146 is referred to as Case 3. In Case 3, wave height was measured at wg2, wg3 and wg5, and horizontal velocity
147 was measured at wg3.

148

149 **3. Results**

150 **3.1.** ***Solitary waves***

151 For the validation of the modified FDS equation using the theoretical solutions of surface solitary waves,
152 the total number of horizontal meshes was given as 1000 with a mesh size of 0.04 m across the whole
153 computational domain, and a time step of 0.00005 s was used with a total time step of 20 s. CFL was estimated
154 to be about 360, which is small enough to carry out computations accurately. Regarding the value of N that
155 determines the computational accuracy, N was given as 3 by following Nakayama and Kakinuma (2010) and
156 Nakayama et al. (2019a) which shows that N=3 can provide accurate enough computational results even under
157 deep-water waves. Regading the value of μ, we gave μ = 2.5. Please see "4. Discussion" for more details,
158 including discussion of the effect of N on the computational accuracy. Seven different wave heights normalized
159 by total water depth were given from about 0.09 to 0.6 with an interval of 0.085. The wave speed of solitary

160 waves agrees well with the theory in Fenton (1972) and becomes slightly smaller than in the KdV theory with
161 the increase in wave height (Solid lines in Fig. 3a). On the other hand, the larger the wave height, the larger
162 the effective wavelength compared to the KdV theory (Solid lines in Fig. 3b). The modified FDS equation
163 successfully reproduced not only the relationship between the normalized wave height and wave speed but
164 also the relationship between the normalized wave height and effective wavelength (Fig. 3). Therefore, the
165 validity of the modified FDS equation was approved through comparisons with theoretical solutions.

166

167 **3.2.** ***Waves without current***

168 The total number of horizontal meshes was given as 500 with a mesh size of 0.05 m across the whole
169 computational domain, and a time step of 0.0005 s was used with a total time step of 50 s. A timeseries of
170 wave heights at the left end was given using a timeseries of measured wave height at wg1. To give similar
171 conditions as the laboratory experiments, a wave absorber was given at the right end with a length of 10 m in
172 order to prevent progress waves from reflecting. *N* was given as 3 the same as solitary wave case. Since fine
173 sediment with a diameter of 0.21 mm was used at the bottom of the tank, bottom friction loss of momentum
174 was considered in the numerical computations (Eq.(24)). In this study, f=0.052 was decided on by changing
175 the value of f by trial and error.

$$momentum\ loss = -\rho \frac{f_c}{h} |u_b| u_b \tag{24}$$

176 where, u_b is the velocity at the bottom, and f_c is the coefficient of energy loss at the bottom.

177 In the computation, 5 different values of μ was applied in the modified FDS equation, 1.0, 1.5, 2.0, 2.5
178 and 3.0. But, the larger the μ given, the more unstable the numerical computation becomes. In Case 2, the
179 condition of μ = 3.0 was very unstable and we could not obtain the results. Therefore, there are 4 different
180 conditions, μ = 1.0, 1.5, 2.0 and 2.5, in Case 2.

181 In Case 1, the wave height at wg2 agrees very well for all the computational results because wg2 is located
182 close to wave generator wg1 (Figs. 4 and 5). In contrast to wg2, the FDS equation slightly overestimated wave
183 height at wg3 when μ = 1.0, and the modified FDS equation underestimated wave height less than μ = 1.0
184 when μ = 3.0. However, it can be said that wave heights from all the computational cases agree well with
185 laboratory experiments. On the other hand, there were large differences between numerical computations and

laboratory experiments for velocity at wg3. When μ = 1.0 (corresponding to the FDS equation), horizontal velocity was overestimated by a factor of two compared to the laboratory experiments (Fig. 4). However, when μ > 1.0 (corresponding to the modified FDS equation), horizontal velocity was estimated to be close to the laboratory experiments, with best agreement when μ = 2.5 (Fig. 5). Interestingly, opposite to horizontal velocity, vertical velocity was underestimated, with the velocity 1/3 of the laboratory experiments when μ = 1.0 (the FDS equation). When μ > 1.0 (the modified FDS equation), vertical velocity estimates were close to the laboratory experiments with the best estimation obtained when μ = 2.5 and vertical velocity overestimated when μ = 3.0.

In Case 2, where the wave height is larger and wave period longer than Case 1, wave height was slightly overestimated at wg3 and wg4 when μ = 1.0 (the FDS equation), which is like Case 1 (Fig. 6). When μ > 1.0 (the modified FDS equation), wave height was estimated very well and the best estimation was found when μ = 2.5 (Fig. 7). Similar to Case 1, horizontal velocity was overestimated at wg3 largely when μ = 1.0, but horizontal velocity was estimated close to the laboratory experiments when μ > 1.0. The best agreements were found when μ = 2.0 or μ = 2.5. Therefore, there may be the possibility that the FDS equation overestimates horizontal velocity and underestimates vertical velocity when μ = 1.0. On the other hand, when μ > 1.0 (the modified FDS equation), horizontal and vertical velocities were estimated very well, with the best agreement when μ = 2.5. This may thus suggest that the application of the modified FDS equation is recommended.

3.3. *Waves with current*

In the analysis for wave-current conditions, it was considered appropriate to apply μ = 2.5 based on the results obtained under the wave condition without current shown in the previous section. Therefore, we applied μ = 2.5 into Case 3 under conditions of wave heights of 0.10 m and the wave periods of 1.0 s against a current of 0.02 m/s. For all the wave gauge stations, wave heights at wg2, wg3 and wg5 were found to agree with the laboratory experiments very well (Fig. 8). Also, horizontal velocity was estimated through the numerical computation, although it gave slightly larger velocities. In comparison with Case 1 (wave without current but the wave height and wave period conditions are the same as Case 3), wave heights under Case 3 at wg3 over

212 a bump were found to be smaller due to the current effect. It is apparent that the amplitude of horizontal
213 velocity was smaller than Case 1 while the mean horizontal velocity was confirmed to be 0.02 m/s smaller
214 than Case 1, which is the effect of the constant 0.02 m/s opposing current.

215

216 **4. Discussion**

217 For evaluating the modified FDS equation, the linearized modified FDS equation were obtained to
218 investigate the dispersion relationship from the viewpoint of changes in μ and *N*. Eqs. (25) and (26) can be
219 obtained by linearizing Eqs. (13) and (14).

$$H^{\mu\alpha}\frac{\partial\eta}{\partial t}+\frac{H^{\mu(\alpha+\beta)+1}}{\mu(\alpha+\beta)+1}\frac{\partial^2 f_\beta}{\partial x^2}-\frac{\mu^2\alpha\beta}{\mu(\alpha+\beta)-1}H^{\mu(\alpha+\beta)-1}f_\beta=0 \tag{25}$$

$$H^{\mu\beta}\frac{\partial f_\beta}{\partial t}+g\eta=0 \tag{26}$$

220 Eq. (27) is obtained from Eqs. (25) and (26).

$$-\frac{\partial^2 f_\beta}{\partial t^2}+\frac{gH}{\mu(\alpha+\beta)+1}\frac{\partial^2 f_\beta}{\partial x^2}-\frac{\mu^2\alpha\beta}{\mu(\alpha+\beta)-1}\frac{g}{H}f_\beta=0 \tag{27}$$

221 The following relationships are obtained by applying small amplitude surface waves.

$$f_\beta=G_\beta\exp[\sigma t-kx] \tag{28}$$

222 Substituting Eq. (28) into Eq. (27) provides Eq. (29).

$$\sigma^2-\frac{gH}{\mu(\alpha+\beta)+1}k^2-\frac{\mu^2\alpha\beta}{\mu(\alpha+\beta)-1}\frac{g}{H}=0 \tag{29}$$

223 where, k is the wave number, and σ is the frequency.

224 The theoretical solution of the dispersion relationship for surface waves, Eq. (30), was compared with the
225 linearized modified FDS equation, Eq. (29) (Fig. 9). We applied 9 different μ (=1.0, 1.5, 2.0, 2.5, 3.0, 3.5, 4.0,
226 4.5, 5.0) and 5 different *N* (=1, 2, 3, 4, 5).

$$c^2 \frac{1}{{c_0}^2} = \left(\frac{\sigma}{k}\right)^2 \frac{1}{gh} = \frac{1}{kh}\tanh(kh) \tag{30}$$

When μ = 1.0 (the FDS equation), solitary-like wave conditions were found to be satisfied by giving N = 3 ($0 < kh < 1$). However, N needs to be larger than 3 to satisfy deep water wave conditions (μ =1.0). For μ =1.5 and μ =2.0, the lines of N = 2 become closer to the theoretical solution compared to μ = 1.0 though N also needs to be larger than 3 to satisfy deep water wave conditions. Interestingly, when μ = 2.5, the lines of N = 3 agree with the theoretical solution very well. The lines when N is larger than 2 for μ = 2.5 agree with the theoretical solutions for not only shallow water conditions but also deep-water conditions. Comparison with the laboratory experiments demonstrated that the computational results agree very well when μ = 2.5, which may suggest that the best recommended value of μ may be 2.5.

On the other hand, when μ = 3.0, results appeared similar to μ = 2.5. However, there are slight gaps when kh was less than 1.0. When μ was more than 3.0, it was more apparent that Eq. (29) cannot agree with the theoretical solution when kh is less than 1.0, though deep-water conditions are satisfied even when N = 2. It is thus revealed that the larger the value of μ, the more the deep-water conditions are satisfied (though shallow water and solitary-like wave conditions cannot be satisfied). Therefore, from the viewpoint of the dispersion relationship and comparisons with laboratory experiments, μ = 2.5 is the recommended value for surface wave computations.

For Case 3 where currents were given against progressive waves, the wave height at wg2 was smaller than in Case 1, which had the same conditions for wave height and wave period without currents. Also, the wave height at wg3 in Case 3 was smaller than Case 1. Dean (1965) and Dalrymple (1974) showed the significant effect of currents on the profile of a surface wave. Since currents against progressive waves were given in Case 3, wave speed in Case 3 is smaller than Case 1, which suggests that wave height becomes smaller resulting in an increase in effective wavelength. Such a larger effective wavelength wave may be categorized as a "bulbous" wave.

In previous studies, when a linear shear or constant opposing current are applied to progressive waves, Teles and Peregrine (1988) suggested that a "bulbous" wave that having a thick or a larger width ridge may

occur. Therefore, as a fundamental analysis, we made an attempt to investigate whether a bulbous wave exists or not using Case 3 where currents are given against progressive waves (Fig. 10). The wavelength of Case 3 was about 1.5 m base on the laboratory experiments and numerical computations, which shows that the wave type is a deep-water wave, kh = 2.1 (kh / (2π) = 0.33 < 1/2) (Mei, 1989). Therefore, we made comparisons with the theoretical solution of a Trochoidal wave which is one of the finite amplitude deep-water waves. It appears that the profile of surface waves computed with the modified FDS equation has a larger width ridge in comparison to the Trochoidal wave (red circle in Fig. 10). However, the apparent bulbous wave only occurred in the region behind the bump, and we could not find a clear bulbous-type wave between the wave generator and the bump. We also investigated only one wave-current interaction case. Therefore, it should be noted that further investigation is necessary to confirm the occurrence of a bulbous wave.

5. Conclusion

The theoretical solution of the dispersion relationship for surface waves was compared with the linearized modified FDS equation, which demonstrated the high applicability of the FDS equation when μ = 2.5. Also, N is recommended to be more than 3 when μ = 2.5 in order to reproduce deep-water waves. By giving μ = 2.5 and N = 3, the modified FDS equation was verified from comparisons with the theoretical solution by Fenton (1972). The modified FDS equation was successfully applied in two laboratory experiments without currents and one laboratory experiment with currents. It was found from the comparisons between with and without current cases that wave height and effective wavelength become smaller and larger, respectively, when a constant opposing current are applied to progressive waves.

Acknowledgements

This work was supported by the Japan Society for the Promotion of Science under grant 18H01545 and 18KK0119.

276 **References**

277 Agnon, Y., Madsen, P. A., Schaffer, H. A. 1999. “A new approach to high-order Boussinesq models.” *J*
278 *Fluid Mech* 399: 319–333.

279 Dalrymple, R.A. 1974. “A finite amplitude wave on a linear shear current.” *J Geophys Res.* 79: 4498-4504.

280 Dean, R.G. 1965. “Stream function representation of nonlinear ocean waves.” *J Geophys Res.* 70 (18): 4561-
281 4572.

282 Grimshaw R. 1971. “The solitary wave in water of variable depth. Part 2.” *J Fluid Mech* 46: 611-622.

283 Fenton J. 1972. “A ninth-order solution for the solitary wave.” *J Fluid Mech* 53: 257-271.

284 Horn, D. A., Redekopp, L.G., Imberger, J., Ivey, G.N. 2000. “Internal wave evolution in a space-time
285 varying field.” *J Fluid Mech* 424: 279-301.

286 Horn, D.A., Imberger, J., Ivey, G.N. 2001. “The degeneration of large-scale interfacial gravity waves in
287 lakes.” *J Fluid Mech* 434: 181–207.

288 Horn, D.A., Imberger, J., Ivey, G.N., Redekopp, L.G. 2002. “A weakly nonlinear model of long internal
289 waves in closed basins.” *J Fluid Mech* 467: 269-287.

290 Isobe, M. 1995. “Time-dependent mild-slope equations for random waves.” *Proc 24th Int Conf Coast Eng*
291 *ASCE*: 285-299.

292 Koop, C.G., Butler, G. 1981. “An investigation of internal solitary waves in a two-fluid system.” *J Fluid*
293 *Mech* 112: 225–254.

294 Madsen, O.S., Mei, C.C. 1969. “The transformation of a solitary wave over an uneven bottom.” *J Fluid*
295 *Mech* 39(4): 781-791.

296 Madsen, P.A., Murray, R., Sorensen, O.R. 1991. “A new form of Boussinesq equations with improved linear
297 dispersion characteristics.” *Coast Eng* 15: 371-388.

298 Madsen, P.A., Sorensen, O.R. 1992. "A new form of Boussinesq equations with improved linear dispersion
299 characteristics. Part 2. A slowly varying bathymetry.” *Coast Eng* 18: 183-204.

300 Maxworthy, T. 1980. ”On the formation of nonlinear internal waves from the gravitational collapse of mixed
301 regions in two and three dimensions.” *J Fluid Mech* 96: 47-64.

302 Mei, C.C. 1989. ”The applied dynamics of ocean surface waves. Advanced Series on Ocean Engineering.”
303 *World Scientific* 1: 768.

304 Mei, C.C., Le, Mehaute, B. 1966. "Note on the Equations of Long Waves Over an Uneven Bottom." *J Geophys*
305 *Res* 71(2): 393-400.
306 Li, W., Yeh, H., Kodama, Y. 2011. "On the Mach reflection of a solitary wave: revisited." *J Fluid Mech* 672:
307 326-357.
308 Luke, J.C. 1967. "A variational principle for a fluid with a free surface." *J Fluid Mech* 27: 395-397.
309 Miles, J.W. 1997a. "Obliquely interacting solitary waves." *J Fluid Mech* 79: 157-169.
310 Miles, J.W. 1997b. "Resonantly interacting solitary waves." *J Fluid Mech* 79: 171-179.
311 Nakayama, K. 2006. "Comparisons of using CIP, compact and CIP-CSL2 schemes for internal solitary waves."
312 *Inter. J. Num. Method. Fluid.* 51: 197–219.
313 Nakayama, K., Kakinuma, T. 2010. "Internal waves in a two-layer system using fully nonlinear internal-
314 wave equations." *Int J Numer Meth Fluids* 62: 574-590.
315 Nakayama, K., Shintani, T., Kokubo, K., Maruya, Y., Kakinuma, T., Komai, K. and Okada, T. 2012.
316 "Residual current over a uniform slope due to breaking of internal waves in a two-layer system." *J.*
317 *Geophy. Res.* 117, C10002. doi: 10.1029/2012JC008155.
318 Nakayama, K., Kakinuma, T., Tsuji, H. 2019a. "Oblique reflection of large internal solitary wave." *Eur. J.*
319 *Mech.* (B), Vol.74: 81-91.
320 Nakayama, K., Lamb, K. 2019c. "Breathers in a three-layer fluid." *J Fluid Mech* submitted.
321 Nakayama, K., Sato, T., Shimizu, K. and L. Boegman. 2019b. "Classification of internal solitary wave
322 breaking over a slope." *Physical Review Fluids*, Vol.4, 014801
323 Nwogu, O. 1993. "An alternative form of the Boussinesq equations for nearshore wave propagation." *J*
324 *Waterw Port Coast Ocean Eng.* 119(6): 618-638.
325 Perigrine, D.H. 1967. "Long waves on a beach." *J Fluid Mech* 27(4): 815-827.
326 Tanaka, M. 1993. "Mach reflection of a large-amplitude solitary wave." *J Fluid Mech* 248: 637-661.
327 Teles, da, Silva, A.F., Peregrine, D. 1988. "Steep steady surface waves on water of finite depth with constant
328 vorticity." *J Fluid Mech* 195: 281-302.
329 Thuy, Thi, Thu, Vu. 2013. "Aspects of inlet geometry and dy-namics." *The University of Queensland, Ph. D.*
330 *Thesis.*

Wei, G., Kirby, J.T. 1995. “A time-dependent numerical code for the extended Boussinesq equations.” *J Waterw Port Coast Ocean Eng* 121(5): 251-261.

Wei, G., Kirby, J.T., Grilli, S.T. and Subramanya, R. 1995. “A fully nonlinear Boussinesq model for surface waves. Part 1. Highly nonlinear unsteady waves.” *J Fluid Mech* 294: 71–92.

Wei, G., Kirby, J.T., Sinha, A. 1999. “Generation of waves in Boussinesq models using a source function method.” *Coast Eng* 36: 271-299.

Zaman, M.H., Hirayama, K., Hiraishi, T. 2000. “A Boussinesq Model to Study Long Period Waves in a Harbor.” *Rept of Port and Harbour Res. Inst.* 39(4): 25-50.

List of Tables and Figures

376 Table 1 Conditions of laboratory experiment.

	wave height (m)	wave period (s)	current (m/s)	wg1	wg2	wg3	wg4	wg5	ADV horizontal velocity (m/s)	ADV vertical velocity (m/s)
Case 1	0.10	1.0	0	O	O	O	--	--	O	O
Case 2	0.14	1.5	0	O	--	O	O	--	O	--
Case 3	0.10	1.0	-0.02	O	O	O	--	O	O	--

377 O: measured. --: not measured.
378
379

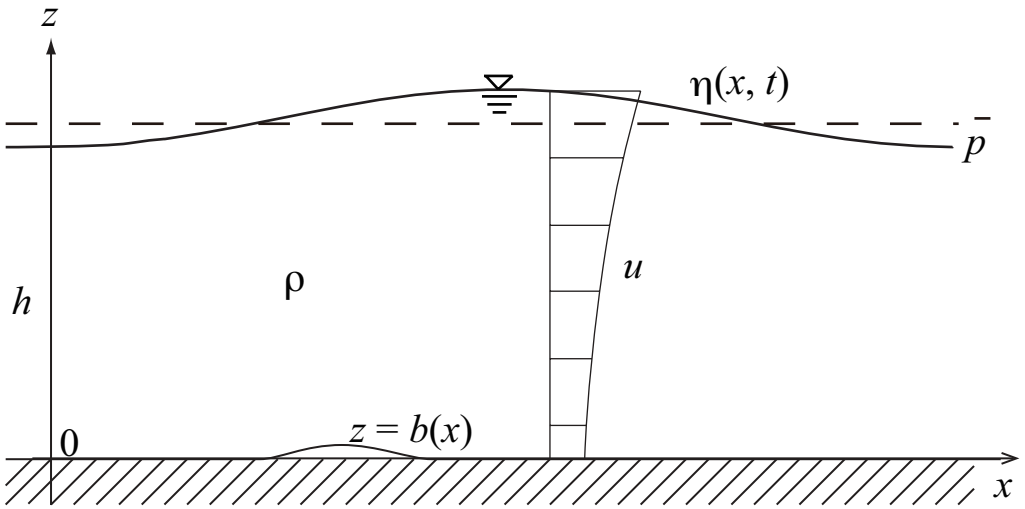

Fig. 1 Schematic diagram of surface waves for the FDS equation.

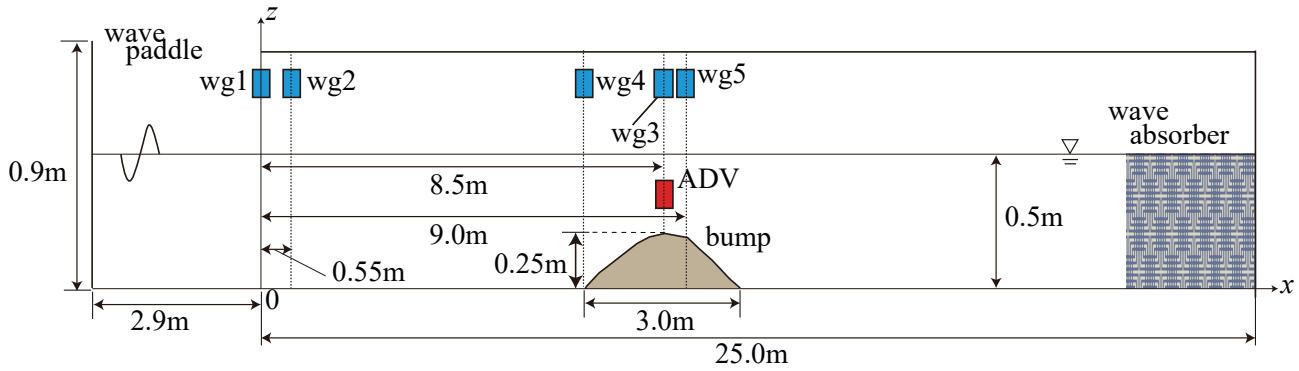

Fig. 2 Open channel tank for laboratory experiment and wave gauge stations and the location of ADV.

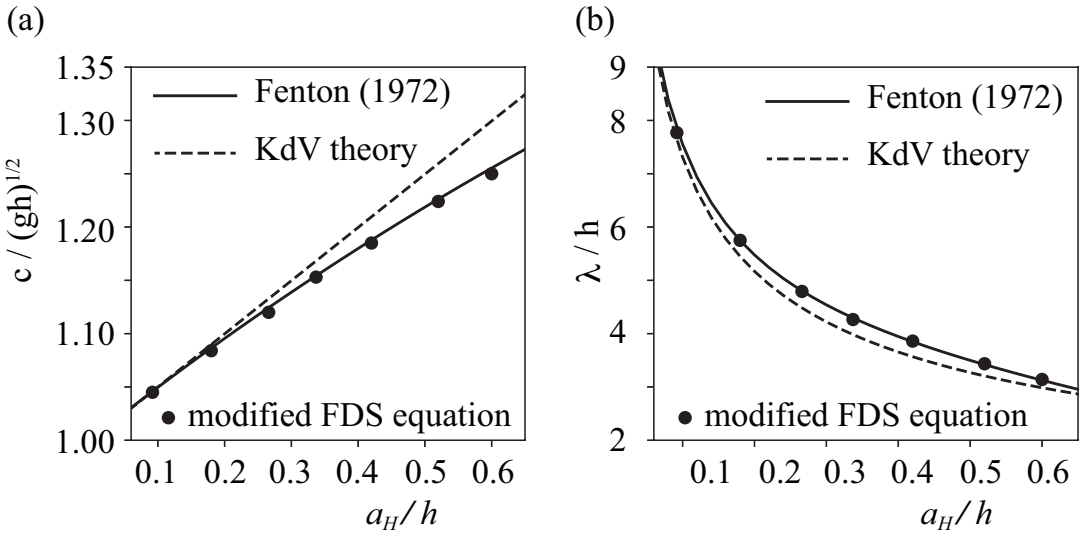

Fig. 3 Comparisons between theoretical solutions and the modified FDS model. (a) Normalized wave height and wave speed. (b) Normalized wave height and wavelength.

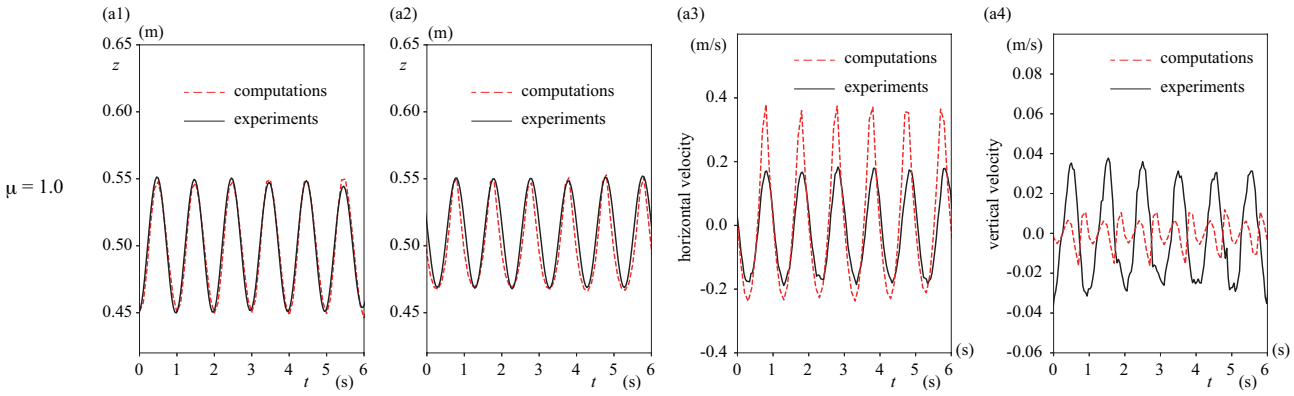

Fig. 4 Comparisons with laboratory experiment case 1 when μ = 1.0. (a1) wave amplitude at wg2. (a2) wave amplitude at wg3. (a3) horizontal velocity at wg3. (a4) vertical velocity at wg3.

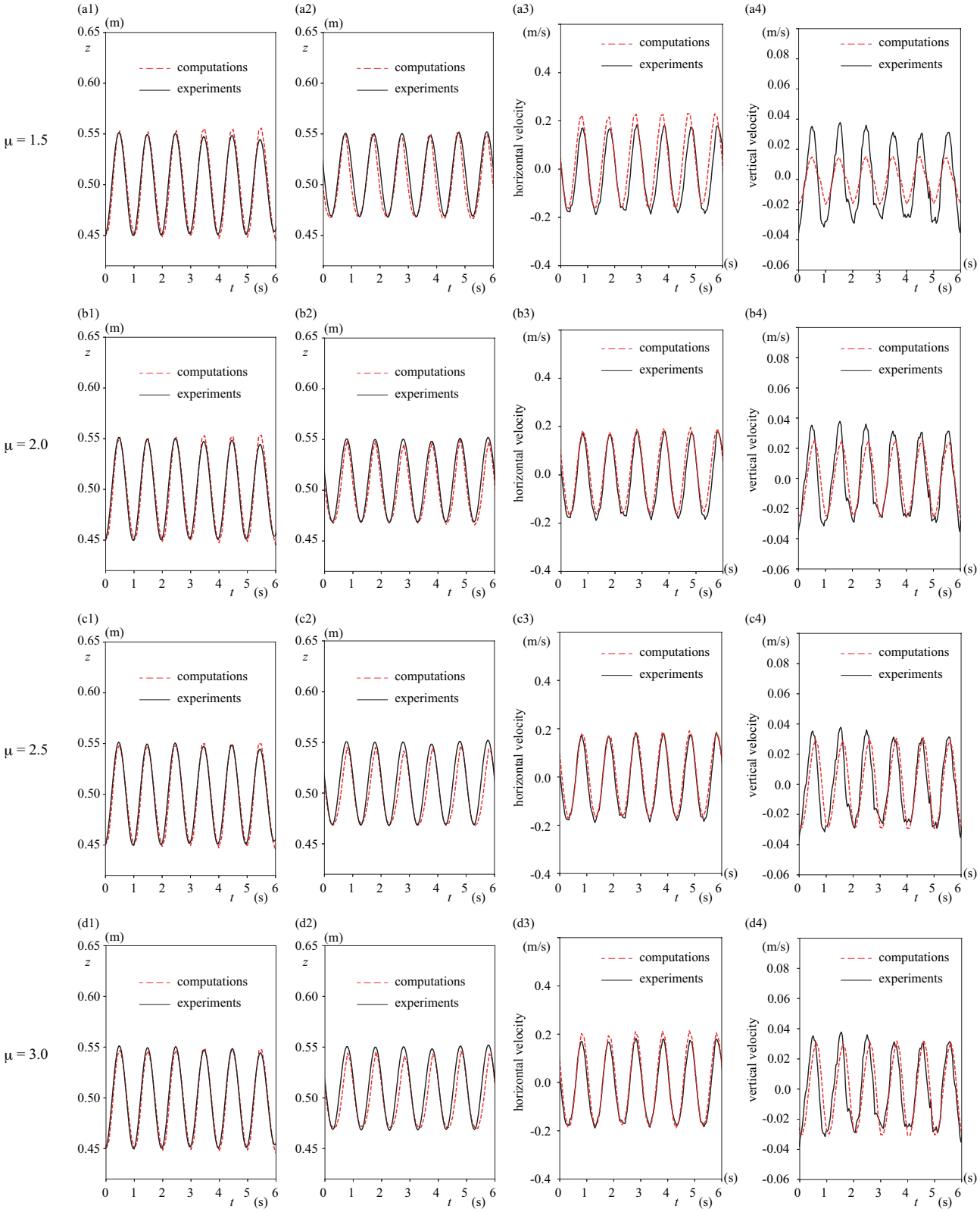

Fig. 5 Comparisons with laboratory experiment case 1 when (a) μ = 1.5, (b) μ = 2.0, (c) μ = 2.5, and (d) μ = 3.0. (a1-d1) wave amplitude at wg2. (a2-d2) wave amplitude at wg3. (a3-d3) horizontal velocity at wg3. (a4-d4) vertical velocity at wg3.

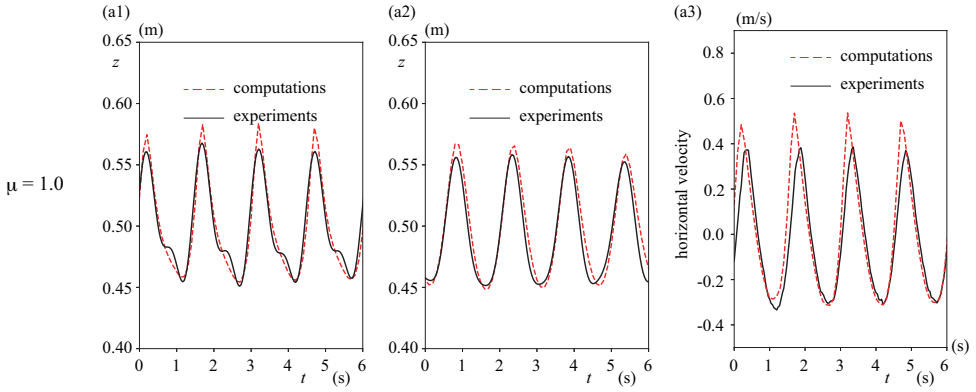

Fig. 6 Comparisons with laboratory experiment case 2 when μ = 1.0. (a1) wave amplitude at wg3. (a2) wave amplitude at wg4. (a3) horizontal velocity at wg3.

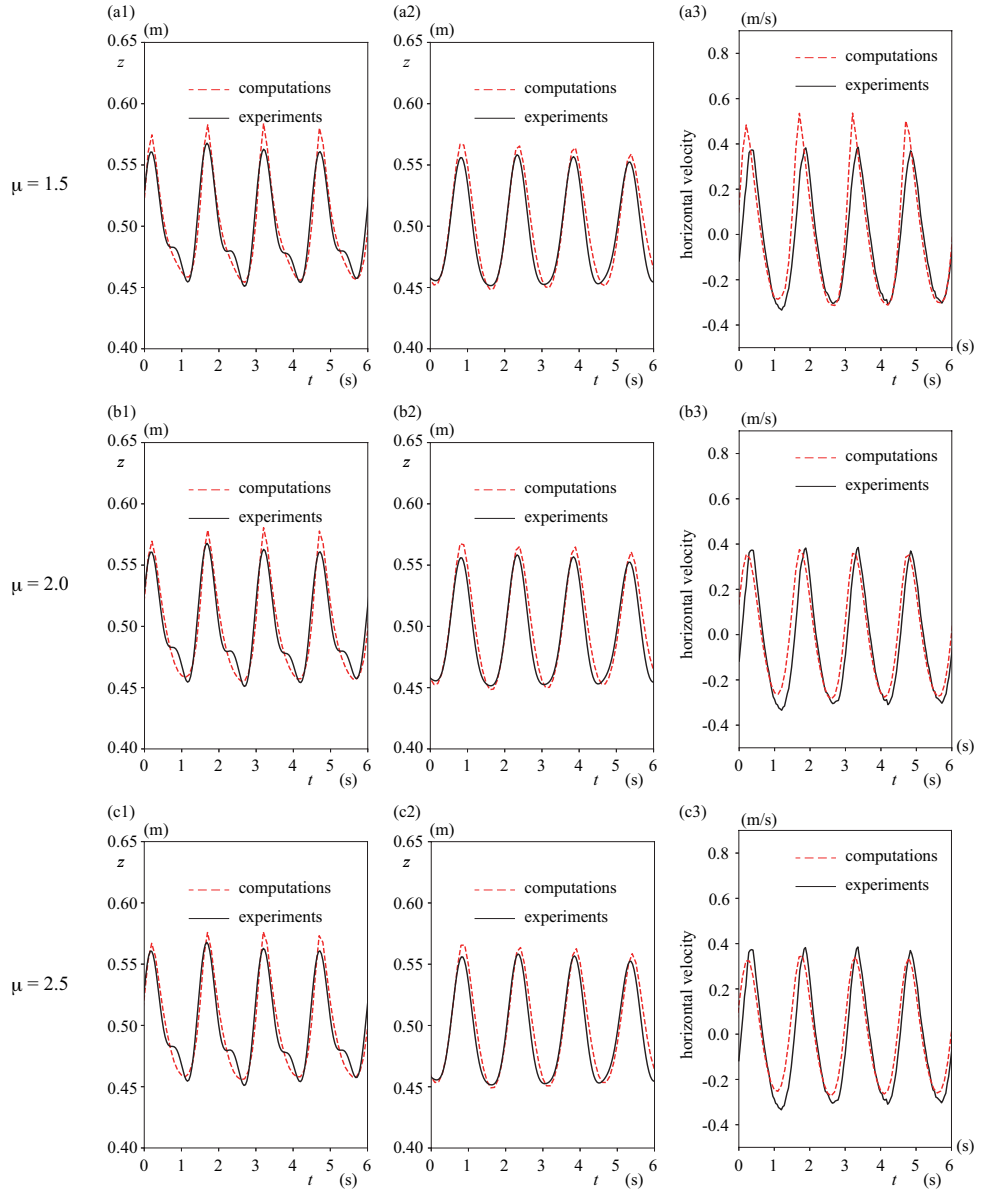

Fig. 7 Comparisons with laboratory experiment case 1 when (a) μ = 1.5, (b) μ = 2.0, and (c) μ = 2.5. (a1-c1) wave amplitude at wg3. (a2-c2) wave amplitude at wg4. (a3-c3) horizontal velocity at wg3.

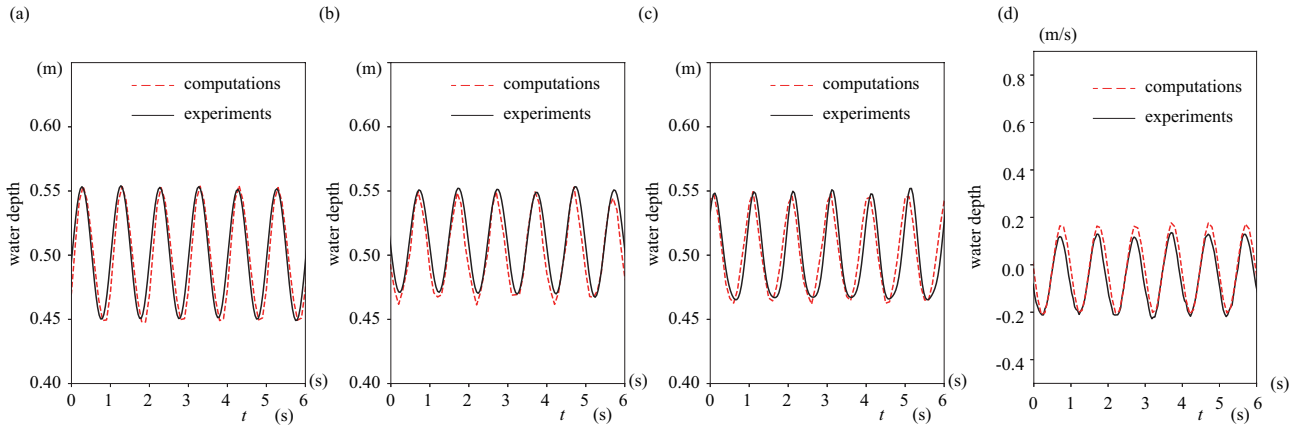

Fig. 8 Comparisons with laboratory experiment case 3 when μ = 2.5. (a) wave amplitude at wg2. (b) wave amplitude at wg3. (c) wave amplitude at wg5. (d) horizontal velocity at wg3.

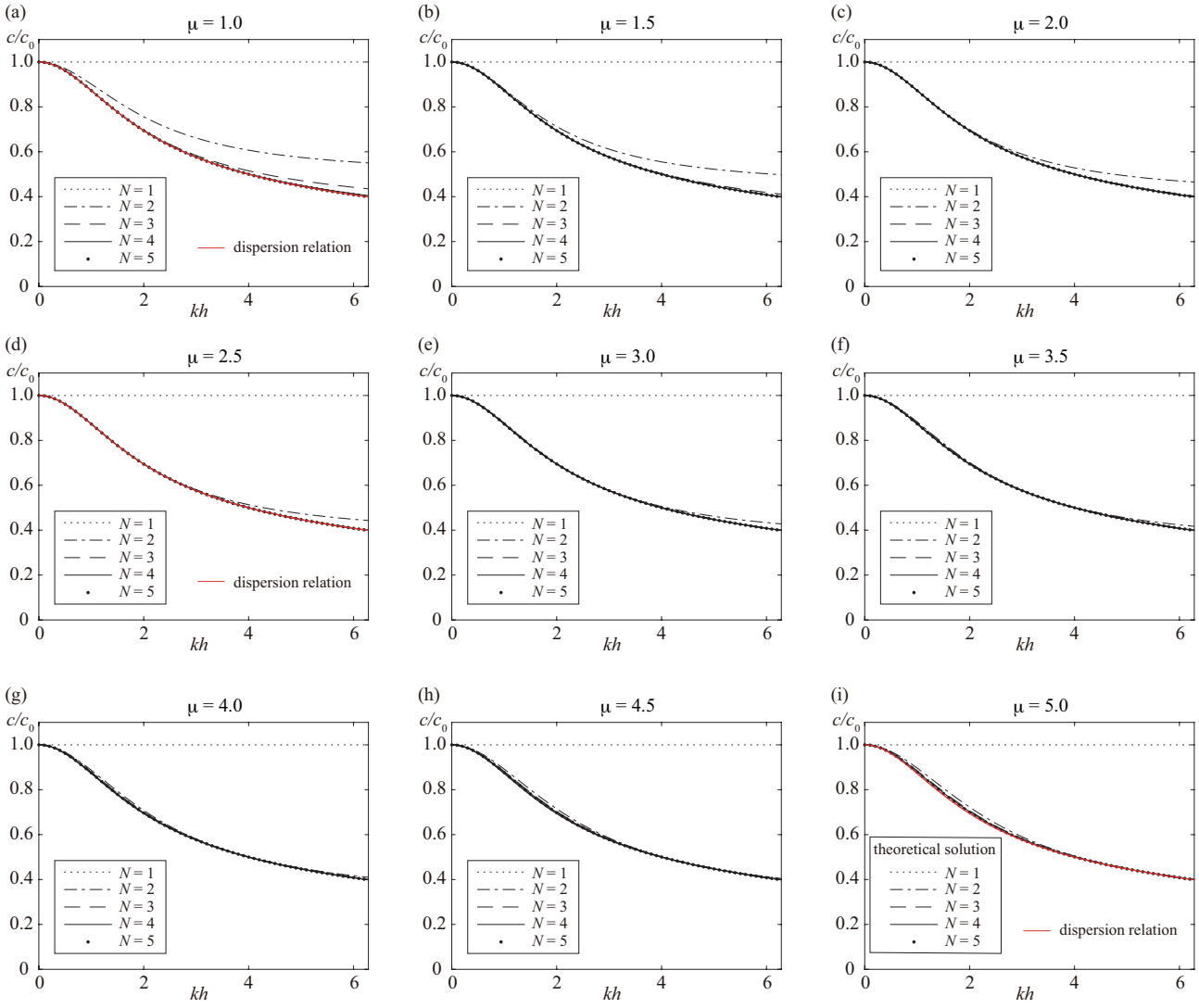

Fig. 9 Dispersion relationship. Red lines indicate the theoretical solution. (a) μ = 1.0, (b) μ = 1.5, (c) μ = 2.0, (d) μ = 2.5, (e) μ = 3.0, (f) μ = 3.5, (g) μ = 4.0, (h) μ = 4.5, and (i) μ = 5.0.

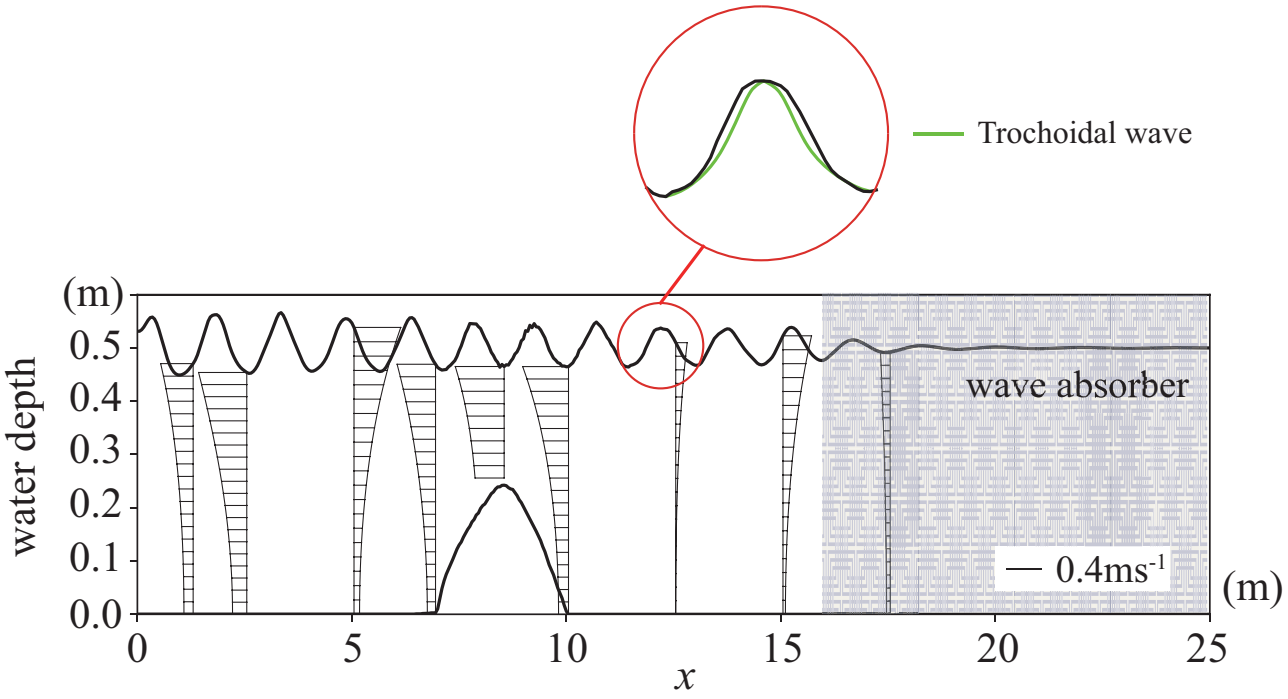

Fig. 10 Wave profile and vertical profile of horizontal velocity in case 3.